Theoretical study of electron-phonon interaction in ZrB_2 and TaB_2

Prabhakar P. Singh*
Department of Physics, Indian Institute of Technology, Powai, Mumbai-400076, India
(Received 9 October 2003; published 25 March 2004)

Using full-potential, density-functional-based methods we have studied electron-phonon interaction in ZrB_2 and TaB_2 in $P6/mmm$ crystal structure. Our results for phonon density of states and Eliashberg function show that the electron-phonon coupling in ZrB_2 is much weaker than in TaB_2. In particular, we find that the average electron-phonon coupling constant λ is equal to 0.15 for ZrB_2 and 0.73 for TaB_2. The solutions of the isotropic Eliashberg gap equation indicate no superconductivity for ZrB_2 but a superconducting transition temperature T_c of around 12 K for TaB_2 with $\mu^* \sim 0.16$.

DOI: 10.1103/PhysRevB.69.094519 PACS number(s): 74.25.Kc, 63.20.Kr

I. INTRODUCTION

The search for superconductivity in the transition-metal diborides ZrB_2 and TaB_2 has proven to be elusive since the first reports of superconductivity in ZrB_2 (Ref. 1) and TaB_2 (Ref. 2) with superconducting transition temperatures $T_c = 5.5$ K and $T_c = 9.5$ K, respectively. The subsequent experimental efforts[3,4] to make ZrB_2 and TaB_2 superconducting by applying external pressure and/or hole doping have also proven to be futile. Such an outcome for ZrB_2 and TaB_2 seems somewhat surprising given that under similar conditions Nb_xB_2 (Ref. 3) and $Mo_{0.96}Zr_{0.04}B_2$ (Ref. 5) are found to superconduct with $T_c = 8.5$ K and $T_C = 5.9$ K, respectively.

To be able to understand the superconducting properties or thereof lack of the transition-metal diborides ZrB_2 and TaB_2 within the conventional BCS theory of superconductivity one needs to know the electron-phonon interaction in these systems. In particular, the strength of the electron-phonon interaction in ZrB_2 and TaB_2, as reflected in the average electron-phonon coupling constant λ, can be used to predict the possibility of superconductivity in the diborides. Experiments, based on point-contact spectroscopy,[6,7] indicate λ to be less than 0.1 for both ZrB_2 and TaB_2, and thus preclude the possibility of superconductivity in these diborides. Here, we like to point out that the experimental determination of λ, as carried out in Refs. 6,7, is more reliable for ZrB_2 than for TaB_2.

Previous theoretical estimates of λ,[4,8] based on only zone-center sampling of the electron-phonon matrix elements, also indicate ZrB_2 and TaB_2 to have a weak electron-phonon coupling with $\lambda < 0.2$. However, it turns out that in the transition-metal diborides the estimates of λ based on zone-center sampling of the electron-phonon matrix elements corresponding to the optical E_{2g} mode is not reliable.[9,10] Thus, a detailed analysis of the electron-phonon interaction using a more representative Brillouin zone sampling of the electron-phonon matrix elements is clearly needed to better understand the lack of superconductivity in ZrB_2 and TaB_2. The present work is a step in that direction.

Using density-functional-based methods we have studied (i) the electronic structure, (ii) the phonon density of states (DOS), (iii) the electron-phonon interaction, and (iv) the solutions of the isotropic Eliashberg gap equation for ZrB_2 and TaB_2 in $P6/mmm$ crystal structure. We have calculated the electronic structure of ZrB_2 and TaB_2 with experimental lattice constants[4,8] a and c, as given in Table I, using full-potential linear muffin-tin orbital (LMTO) method. For studying the electron-phonon interaction we used the full-potential linear-response program of Savrasov[11,12] to calculate the dynamical matrices and the Hopfield parameters, which were then used to calculate the phonon DOS, $F(\omega)$, the electron-phonon coupling λ, including the partial $\lambda_{\mathbf{q}}$, and the Eliashberg function, $\alpha^2F(\omega)$, for ZrB_2 and TaB_2. Subsequently, we have numerically solved the isotropic Eliashberg gap equation[13–15] for a range of μ^*, the Coulomb pseudopotential, to obtain the corresponding superconducting transition temperature T_c.

Based on our calculations, described below, we find that the electron-phonon coupling in ZrB_2 is much weaker than in TaB_2. In particular, we find that the average electron-phonon coupling constant λ is equal to 0.15 for ZrB_2 and 0.73 for TaB_2. The solutions of the isotropic Eliashberg gap equation indicate no superconductivity for ZrB_2 but a superconducting transition temperature T_c of around 12 K for TaB_2 with $\mu^* \sim 0.16$.

II. THEORETICAL APPROACH AND COMPUTATIONAL DETAILS

Within Migdal-Eliashberg theory of superconductivity,[13,14] first-principles calculations of superconducting properties require the knowledge of (i) the ground-state electronic structure, (ii) the vibrational spectrum, and (iii) the electron-phonon matrix elements of the solid. The phonon spectrum and the electron-phonon matrix elements are then used to calculate the Eliashberg functions from which the superconducting properties of the materials can be calculated. In particular, by solving the fully anisotropic or the

TABLE I. The experimental lattice constants for ZrB_2 and TaB_2 used in the calculations.

Alloy	a (a.u.)	c/a
ZrB_2	5.992	1.1142
TaB_2	5.826	1.0522

isotropic gap equation the superconducting transition temperature can be calculated.

The density-functional theory provides a reliable framework for implementing from first principles the Migdal-Eliashberg approach for calculating the superconducting properties of metals as outlined above. Such an approach has been implemented by Savrasov using the LMTO formalism and the linear response method, the details of which are given in Refs. 11,12. In the following, we briefly outline the approach used in the present calculations. We follow the notation used in Refs. 11,12.

We calculate the ground-state electronic structure of the transition-metal diborides ZrB_2 and TaB_2 using the full-potential linear muffin-tin orbital method in the generalized-gradient approximation of the density-functional theory. The linear-response approach is used to evaluate the dynamical matrices and the electron-phonon matrix elements within the density-functional theory as implemented using the LMTO formalism. It amounts to self-consistently evaluating the changes in the electronic structure due to atomic displacements associated with the phonon mode $\omega_{\mathbf{q}\nu}$. Once the changes in the wave function, density, and the effective potential are known, the phonon density of states

$$F(\omega)=\sum_{\mathbf{q}\nu}\delta(\omega-\omega_{\mathbf{q}\nu}), \tag{1}$$

and the electron-phonon matrix elements

$$g^{\mathbf{q}\nu}_{\mathbf{k}+\mathbf{q}j',\mathbf{k}j}=\langle \mathbf{k}+\mathbf{q}j'|\,\delta^{\mathbf{q}\nu}V_{eff}|\mathbf{k}j\rangle \tag{2}$$

can be evaluated. The electron-phonon matrix elements can be interpreted as the scattering of electron in state $|\mathbf{k}j\rangle$ to state $|\mathbf{k}+\mathbf{q}j'\rangle$ due to perturbing potential $\delta^{\mathbf{q}\nu}V_{eff}$, which arises due to the phonon mode $\omega_{\mathbf{q}\nu}$. Note that Eq. (2) has to be corrected for the incomplete basis set as described in Ref. 11. From the electron-phonon matrix elements we can calculate the phonon linewidth $\gamma_{\mathbf{q}\nu}$,

$$\gamma_{\mathbf{q}\nu}=2\pi\omega_{\mathbf{q}\nu}\sum_{\mathbf{k}jj'}|g^{\mathbf{q}\nu}_{\mathbf{k}+\mathbf{q}j',\mathbf{k}j}|^2\delta(\epsilon_{\mathbf{k}j}-\epsilon_F)\,\delta(\epsilon_{\mathbf{k}+\mathbf{q}j'}-\epsilon_F). \tag{3}$$

Occasionally, it is useful to define a phonon mode dependent electron-phonon coupling $\lambda_{\mathbf{q}\nu}$ as

$$\lambda_{\mathbf{q}\nu}=\frac{\gamma_{\mathbf{q}\nu}}{\pi N(\varepsilon_F)\omega^2_{\mathbf{q}\nu}}, \tag{4}$$

where $N(\varepsilon_F)$ is the electronic density of states at the Fermi energy. Now we can combine the electronic density of states, phonon spectrum, and the electron-phonon matrix elements to obtain the Eliashberg function $\alpha^2F(\omega)$ defined as

$$\alpha^2F(\omega)=\frac{1}{2\pi N(\epsilon_F)}\sum_{\mathbf{q}\nu}\frac{\gamma_{\mathbf{q}\nu}}{\omega_{\mathbf{q}\nu}}\delta(\omega-\omega_{\mathbf{q}\nu}). \tag{5}$$

Finally, the Eliashberg functions can be used to solve the isotropic gap equation[13–15]

$$\Delta(i\omega_n)=\sum_{n'}^{|\omega_{n'}|<\omega_c} f_{n'}S(n,n')\Delta(i\omega_{n'}) \tag{6}$$

to obtain the superconducting properties such as the superconducting transition temperature T_c. The function $S(n,n')$ used in the gap equation is defined by

$$S(n,n')\equiv\lambda(n-n')-\mu^*-\delta_{nn'}\sum_{n''}s_ns_{n''}\lambda(n-n'') \tag{7}$$

and $f_n=1/|2n+1|$ with s_n representing the sign of ω_n. The electron-phonon coupling $\lambda(\nu)$ is given by

$$\lambda(\nu)=\int_0^\infty d\omega\alpha^2F(\omega)\frac{2\omega}{\omega_\nu^2+\omega^2}. \tag{8}$$

Before describing our results in detail, we provide some of the computational details which are similar to our study of the electron-phonon interaction in MgB_2, NbB_2, and TaB_2.[10,9]

The charge self-consistent full-potential linear muffin-tin orbital calculations were carried out with the generalized gradient approximation for exchange correlation of Perdew *et al.*[16,17] and 484 **k** points in the irreducible wedge of the Brillouin zone. For TaB_2, the basis set used consisted of *s*, *p*, *d*, and *f* orbitals at the Ta site and *s*, *p*, and *d* orbitals at the B site. In the case of ZrB_2, we included *s*, *p*, and *d* orbitals at the Zr site. In all cases the potential and the wave function were expanded up to $l_{max}=6$. The muffin-tin radii for Ta, B, and Zr were taken to be 2.5, 1.66, and 2.3 a.u., respectively.

The calculation of dynamical matrices and the Hopfield parameters for ZrB_2 and TaB_2 were carried out using a $6\times6\times6$ grid resulting in 28 irreducible **q** points. The Brillouin zone integrations for charge self-consistency during linear-response calculations were carried out using a $12\times12\times12$ grid of **k** points. The Fermi surface was sampled more accurately with a $36\times36\times36$ grid of **k** points using the double grid technique as outlined in Ref. 12. In case of TaB_2, for a couple of **q** points we had to sample the Fermi surface using a $48\times48\times48$ grid of **k** points to get converged acoustic-mode frequencies.

III. RESULTS AND DISCUSSION

In this section we describe the results of our calculations of the electronic structure, the linear response, and the solutions of the isotropic Eliashberg gap equation for ZrB_2 and TaB_2. Our results for ZrB_2 and TaB_2 are described in terms of (i) the DOS, (ii) the phonon density of states $F(\omega)$, (iii) the Eliashberg function $\alpha^2F(\omega)$, and (iv) the superconducting transition temperature T_c obtained from the solutions of the isotropic Eliashberg gap equation.

A. The density of states

The electronic structure of ZrB_2 (Refs. 8,18) and TaB_2 (Refs. 4,18,19) has been studied previously. Our full-potential results for the electronic structure of ZrB_2 and TaB_2 are in agreement with earlier calculations. For example, in

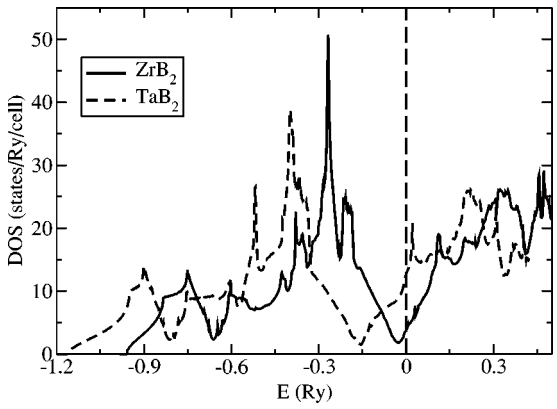

FIG. 1. The total density of states of ZrB_2 and TaB_2 calculated using the full-potential linear muffin-tin orbital method as described in the text. The vertical dashed line indicates the Fermi energy.

Fig. 1 we show the total densities of states for ZrB_2 and TaB_2 calculated at the experimental lattice constants using the full-potential LMTO method as described earlier. The agreement with earlier calculations of the densities of states for ZrB_2 (Ref. 8) and TaB_2 (Ref. 4) is excellent. We find that the total DOS at the Fermi energy is equal to 3.72 st/Ry and 12.52 st/Ry for ZrB_2 and TaB_2, respectively. In ZrB_2, the relatively low DOS at the Fermi energy leads to a weak electron-phonon coupling in this system. However, at the Fermi energy the d electrons are present in substantial amount in both ZrB_2 and TaB_2, indicating a more active role for Zr and Ta atoms in determining the lattice dynamical as well as the possible superconducting properties of these diborides.

B. The phonon density of states

In Fig. 2 we show the phonon DOS $F(\omega)$ of ZrB_2 and TaB_2 calculated using the full-potential linear-response program as described earlier. As is clear from Fig. 2, the phonon DOS for both ZrB_2 and TaB_2 can be separated into three distinct regions. Based on our analysis of the eigenvectors, we find that the first region, with a peak in phonon DOS at 32 meV in ZrB_2 and 22 meV in TaB_2, is dominated by the

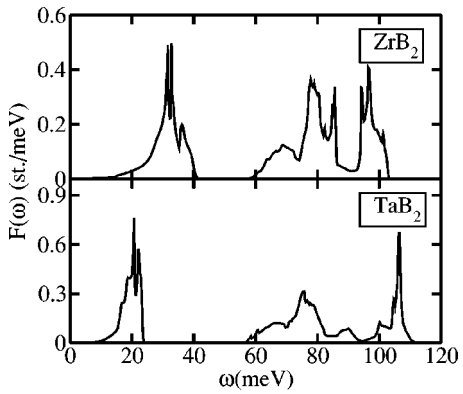

FIG. 2. The phonon density of states $F(\omega)$ of ZrB_2 and TaB_2 calculated using the full-potential linear-response method as described in the text.

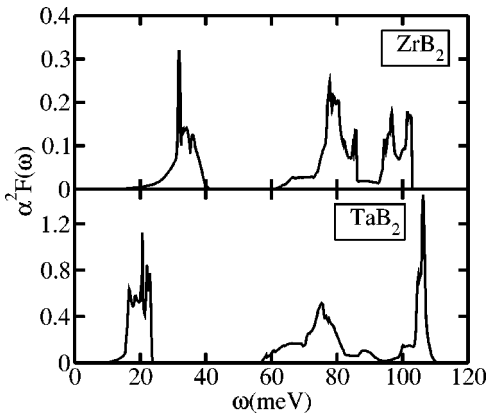

FIG. 3. The Eliashberg function $\alpha^2F(\omega)$ of ZrB_2 and TaB_2 calculated using the full-potential linear-response method as described in the text.

motion of the transition-metal atoms Zr and Ta, respectively. Note that the shift of the first region in the phonon DOS towards lower frequency for TaB_2 in comparison to ZrB_2 is due to the higher mass of Ta. In the second region, the phonon DOS around 60–70 meV in ZrB_2 (TaB_2) results from the coupled motion of Zr (Ta) and the two B atoms. However, the peaks in the phonon DOS at 78 meV in ZrB_2 and 75 meV in TaB_2 correspond to the in-plane B-B motion. The phonon DOS in the third region, which extends from 94 meV to 102 meV in ZrB_2 and from 100 meV to 107 meV in TaB_2, results from the displacements of all the three atoms. Not surprisingly, the phonon DOS of ZrB_2 and TaB_2 are similar to the phonon DOS of NbB_2 if we make allowance for the difference in the masses of the transition-metal atoms.[10]

C. The Eliashberg function

The main purpose of the present study is to examine the strengths of the electron-phonon interaction in ZrB_2 and TaB_2 in order to better understand the lack of superconductivity in these diborides. To this end, we show in Fig. 3 the Eliashberg function $\alpha^2F(\omega)$ of ZrB_2 and TaB_2 calculated as described earlier. A comparison of $\alpha^2F(\omega)$ of ZrB_2 and TaB_2 shows that the electron-phonon coupling in ZrB_2 is much weaker than in TaB_2. In particular, the average electron-phonon coupling constant λ is equal to 0.15 for ZrB_2 and 0.73 for TaB_2.

From Fig. 3, we also see that in the case of ZrB_2 the phonon mode with peak at 78 meV, which corresponds to the in-plane B-B motion, couples to the electrons more than the phonon mode with peak at 32 meV. However, in TaB_2 it is the phonon mode corresponding to the displacements of the transition-metal atom Ta, with a peak at 22 meV, which couples more strongly to the electrons. Such a change in $\alpha^2F(\omega)$ clearly indicates a more active role for the transition-metal atoms in deciding the normal as well as the superconducting state (if any) properties of the transition-metal diborides.

To highlight the contribution made by the transition-metal atoms to the electron-phonon coupling in the transition-metal diborides, we show in Fig. 4 the electron-phonon prefactor

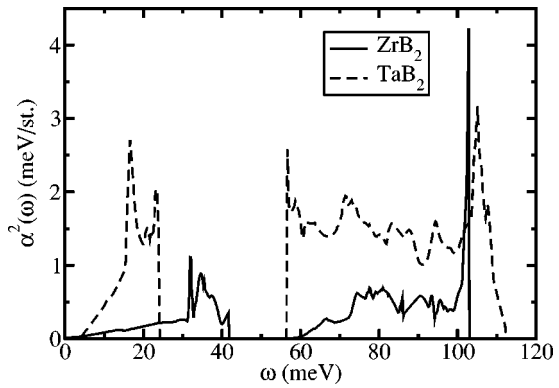

FIG. 4. The prefactor $\alpha^2(\omega)$ of ZrB_2 and TaB_2 calculated using the full-potential linear-response method as described in the text.

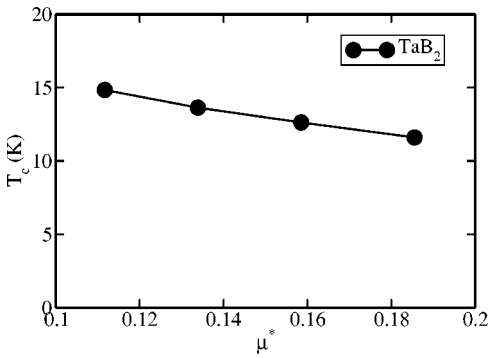

FIG. 5. The superconducting transition temperature T_c as a function of μ^* for TaB_2 as obtained from the isotropic Eliashberg gap equation.

$\alpha^2(\omega)$, defined as the ratio $\alpha^2F(\omega)/F(\omega)$, for ZrB_2 and TaB_2. A comparison of the prefactor $\alpha^2(\omega)$ of ZrB_2 and TaB_2 over their respective modes, as shown in Fig. 4, confirms the enhanced contribution of transition-metal atoms in TaB_2 in comparison to ZrB_2. Note that in ZrB_2 and TaB_2 the phonon modes corresponding to the in-plane B-B motion have peaks in the range of 75–80 meV.

Our calculated $\alpha^2F(\omega)$ for ZrB_2 agrees with the point-contact spectroscopy results of Refs. 6,7. However, in our opinion, the experimentally obtained $\alpha^2F(\omega)$ for TaB_2 in Ref. 7 is underestimated, and it is in disagreement with the present result. In Table II we have listed the Hopfield parameter η, the electron-phonon coupling constant λ, and the various averages of the phonon frequencies for ZrB_2 and TaB_2.

D. The superconducting transition temperature

The possibility of superconductivity in ZrB_2 and TaB_2 within the present approach can be checked by solving numerically the isotropic gap equation[14,15] using the calculated Eliashberg function $\alpha^2F(\omega)$. The results of such a calculation for TaB_2 are shown in Fig. 5 for a range of values of μ^*. From Fig. 5 we find that for $\mu^* \simeq 0.16$ the T_c for TaB_2 is equal to $\sim$12 K. A similar calculation for ZrB_2 using the calculated Eliashberg function yields a T_c of less than 10^{-5} K.

Our results show that ZrB_2 is unlikely to show superconductivity, in agreement with experiments.[20] In addition, the calculated Eliashberg function for ZrB_2 agrees well with the corresponding Eliashberg function obtained from point-contact spectroscopy.[6,7] However, our calculations predict TaB_2 to superconduct with a $T_c \sim 12$ K but so far no superconductivity[3] has been found (except for Ref. 1). Although our calculated values of $\alpha^2F(\omega)$ and consequently λ can be improved upon by including more **q** points in the linear-response calculations but it is unlikely to change the main conclusions of the present work. Thus, the reasons for the lack of superconductivity in TaB_2 need to be explored further.

TABLE II. The calculated Hopfield parameter η, the average electron-phonon coupling constant λ, the root-mean-square ω_{rms}, and the logarithmically averaged ω_{ln} phonon frequencies for ZrB_2 and TaB_2.

Alloy	η (mRy/a.u.^{2})	λ	ω_{rms} (K)	ω_{ln} (K)
ZrB_2	76	0.15	734	585
TaB_2	279	0.73	593	356

E. Convergence of phonon density of states, Eliashberg function and superconducting transition temperature

The first-principles study of superconducting properties of solids as carried out above is computationally demanding. In particular, the requirement of electronic self-consistency for phonon wave vector **q** and mode ν makes the computational effort prohibitive unless one makes a judicious choice of **q** vectors. However, one must ensure that the calculated results are converged with respect to the number of **q** vectors. To demonstrate the convergence of our calculated phonon density of states $F(\omega)$, Eliashberg functions $\alpha^2F(\omega)$, and the superconducting transition temperature T_c, we have carried out two sets of calculations using the double-grid technique as outlined in Refs. 11,12. We have used two **q** grids (i) a $4\times4\times4$ grid with 12 irreducible **q**-points and (ii) a $6\times6\times6$ grid with 28 irreducible **q** points. All the results de-

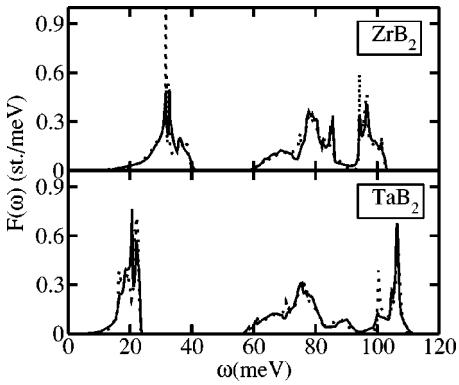

FIG. 6. The phonon density of states $F(\omega)$ of ZrB_2 and TaB_2 obtained with 12 **q** points (dotted line) and 28 **q** points (solid line) using the full-potential linear-response method as described in the text.

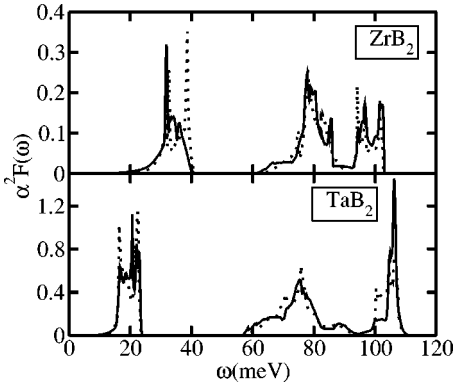

FIG. 7. The Eliashberg function $\alpha^2F(\omega)$ of ZrB_2 and TaB_2 obtained with 12 **q** points (dotted line) and 28 **q** points (solid line) using the full-potential linear-response method as described in the text.

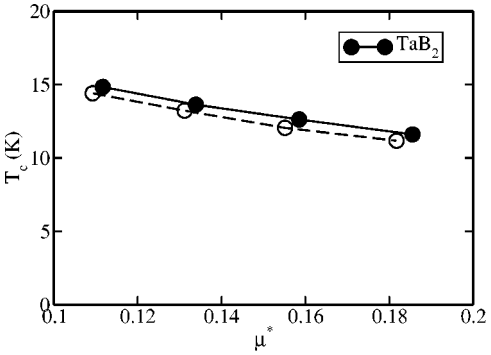

FIG. 8. The superconducting transition temperature T_c as a function of μ^* for TaB_2 as obtained from the isotropic Eliashberg gap equation. The dashed and the solid lines correspond to the calculations done with 12 and 28 **q** points, respectively.

scribed so far correspond to the second grid with 28 **q** points. Below we show a comparison of $F(\omega)$, $\alpha^2F(\omega)$, and T_c calculated using the two grids with 12 and 28 **q** points, respectively.

In Fig. 6 we compare $F(\omega)$ calculated using the two grids with 12 and 28 **q** points, respectively. In general, dynamical matrices and consequently the phonon spectrum do not require a very fine **k** mesh for convergence. However, the increase in the number of **q** points has understandably reduced the peak heights at ω approximately equal to 30 meV, 75 meV, and 95 meV for ZrB_2 and 20 meV, 70 meV, and 100 meV for TaB_2.

The convergence of $\alpha^2F(\omega)$ is shown in Fig. 7, where we have plotted $\alpha^2F(\omega)$ calculated using the two grids with 12 and 28 **q** points, respectively. For ZrB_2 the differences are small in magnitude except at around 20 meV, while for TaB_2 the effects due to small number of **q** points are reduced with the use of the 28 **q**-point grid. We also see that the integrated values such as the electron-phonon coupling constant λ do not change appreciably between the two sets of calculations (λ changes by ~ 0.01 for ZrB_2 and ~ 0.005 for TaB_2).

As $F(\omega)$ and $\alpha^2F(\omega)$ do not change significantly between the two sets of calculations, we do not expect a significant change in the solutions of the isotropic gap equation. Consequently, the calculated T_c should be similar in the two cases. In Fig. 8, we show the T_c obtained for the two sets of calculations, and the difference of less than 1° K between the two sets of calculations confirms the convergence of $F(\omega)$, $\alpha^2F(\omega)$, and T_c.

IV. CONCLUSIONS

We have studied electron-phonon interaction in ZrB_2 and TaB_2 in $P6/mmm$ crystal structure using full-potential, density-functional-based methods. we find that the electron-phonon coupling in ZrB_2 is much weaker than in TaB_2. In particular, we find that the average electron-phonon coupling constant λ is equal to 0.15 for ZrB_2 and 0.73 for TaB_2. The solutions of the isotropic Eliashberg gap equation indicate no superconductivity for ZrB_2 but a superconducting transition temperature T_c of around 12 K for TaB_2 with $\mu^* \sim 0.16$.

*Electronic address: ppsingh@phy.iitb.ac.in

[1] V.A. Gasparov, N.S. Sidorov, I.I. Zver'kova, and M.P. Kulakov, JETP Lett. **73**, 532 (2001).
[2] D. Kaczorowski, A.J. Zaleski, O.J. Zogal, and J. Klamut, cond-mat/0103571 (unpublished).
[3] A. Yamamoto, C. Takao, T. Masui, M. Izumi, and S. Tajima, cond-mat/0208331 (unpublished).
[4] H. Rosner, W.E. Pickett, S.L. Dreschsler, A. Handstein, G. Behr, G. Fuchs, K. Nevkov, K. Muller, and H. Eschring, Phys. Rev. B **64**, 144516 (2001).
[5] L.E. Muzzy, M. Avdeev, G. Lawes, M.K. Haas, H.W. Zandbergen, A.P. Ramirez, J.D. Jorgensen, and R.J. Cava, cond-mat/0206006 (unpublished).
[6] I.K. Yanson, Yu.G. Naidyuk, O.E. Kvitnitskaya, V.V. Fisun, N.L. Bobrov, P.N. Chubov, V.V. Ryabovol, G. Behr, W.N. Kang, E.-M. Choi, H.-J. Kim, S.-I. Lee, T. Aizawa, S. Otani, and S.-L. Drechsler, Mod. Phys. Lett. B **17**, 657 (2003).
[7] Y.G. Naidyuk, O.E. Kvitnitskaya, I.K. Yanson, S.-L. Drechsler, G. Behr, and S. Otani, Phys. Rev. B **66**, 140301 (2002).
[8] H. Rosner, J.M. An, W.E. Pickett, and S.-L. Drechsler, Phys. Rev. B **66**, 024521 (2002).
[9] P.P. Singh, Phys. Rev. B **67**, 132511 (2003).
[10] P.P. Singh, Solid State Commun. **125/6**, 323 (2003).
[11] S.Y. Savrasov, Phys. Rev. B **54**, 16 470 (1996).
[12] S.Y. Savrasov and D.Y. Savrasov, Phys. Rev. B **54**, 16 487 (1996).
[13] P.B. Allen and R.C. Dynes, Phys. Rev. B **12**, 905 (1975).
[14] P. B. Allen and B. Mitrovic, *Solid State Physics: Advances in Research and Applications* (Academic, New York, 1982), Vol. 37, p. 1.
[15] P. B. Allen (private communication).
[16] J.P. Perdew and Y. Wang, Phys. Rev. B **45**, 13 244 (1992).
[17] J.P. Perdewa, K. Burke, and M. Ernzerhof, Phys. Rev. Lett. **77**, 3865 (1996).
[18] I.R. Shein and A.L. Ivanovskii, cond-mat/0109445 (unpublished).
[19] P.P. Singh, cond-mat/0104580 (unpublished).
[20] L. Layarovska and E. Layarovski, J. Less-Common Met. **67**, 249 (1979).